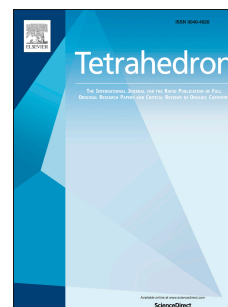


# Accepted Manuscript

Cyclization of  $\beta$ -hydroxyalkylphosphine oxides - mechanism elucidation using experimental and DFT methods

Katarzyna Włodarczyk, Piotr Borowski, Mateusz Drach, Marek Stankevič



PII: S0040-4020(16)31276-5

DOI: [10.1016/j.tet.2016.12.008](https://doi.org/10.1016/j.tet.2016.12.008)

Reference: TET 28300

To appear in: *Tetrahedron*

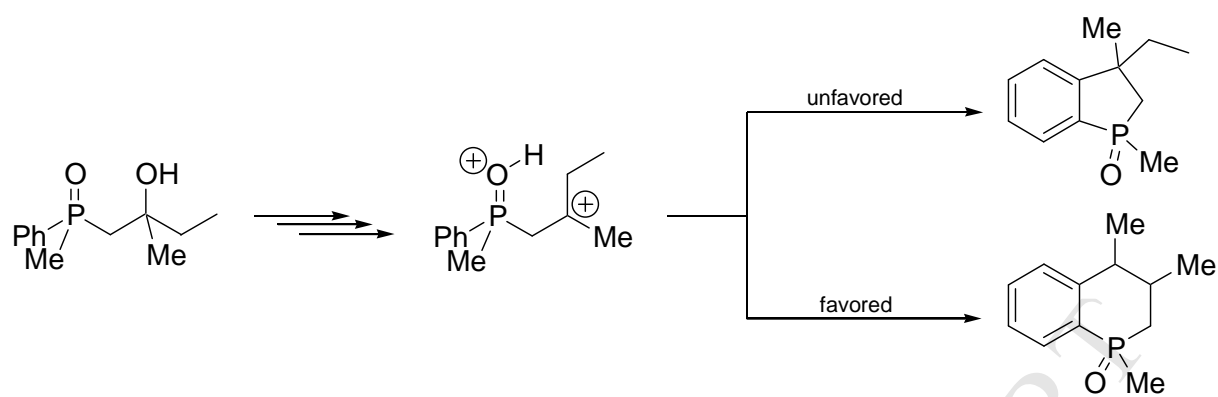
Received Date: 12 September 2016

Revised Date: 19 November 2016

Accepted Date: 6 December 2016

Please cite this article as: Włodarczyk K, Borowski P, Drach M, Stankevič M, Cyclization of  $\beta$ -hydroxyalkylphosphine oxides - mechanism elucidation using experimental and DFT methods, *Tetrahedron* (2017), doi: 10.1016/j.tet.2016.12.008.

This is a PDF file of an unedited manuscript that has been accepted for publication. As a service to our customers we are providing this early version of the manuscript. The manuscript will undergo copyediting, typesetting, and review of the resulting proof before it is published in its final form. Please note that during the production process errors may be discovered which could affect the content, and all legal disclaimers that apply to the journal pertain.



# Cyclization of $\beta$ -hydroxyalkylphosphine oxides - mechanism elucidation using experimental and DFT methods

Katarzyna Włodarczyk,<sup>[a]</sup> Piotr Borowski,<sup>[b]</sup> Mateusz Drach<sup>[c]</sup> and Marek Stankevič<sup>[a]\*</sup>

<sup>[a]</sup> Department of Organic Chemistry, Faculty of Chemistry, Marie Curie-Skłodowska University,  
Gliniana 33, 20-614 Lublin, Poland

<sup>[b]</sup> Department of Chromatographic Methods, Faculty of Chemistry, Marie Curie-Skłodowska  
University, Marie Curie-Skłodowska sq. 3, 20-031 Lublin, Poland

<sup>[c]</sup> Department of Theoretical Chemistry, Faculty of Chemistry, Marie Curie-Skłodowska University,  
Marie Curie-Skłodowska sq. 3, 20-031 Lublin, Poland

\* - Corresponding author. Tel.: +48 81 537-77-52; fax: +48 81 524-22-51;  
email: [marek.stankevic@poczta.umcs.lublin.pl](mailto:marek.stankevic@poczta.umcs.lublin.pl)

## ABSTRACT

$\beta$ -Hydroxyalkylphosphine oxides undergo an intramolecular electrophilic cyclization reaction in strongly acidic media. The main product in cases where rearrangement of the starting  $\beta$ -carbocation is possible possesses the benzophosphorinane skeleton. To gain insight into the mechanism of this transformation, both experimental methods and DFT calculations have been used. The data show a clear dependence of the selectivity of the reaction on both the amount and the concentration of the acid. NMR experiments provided some insight into the transformation of the substrate whereas DFT calculations explain the preferential formation of benzophosphorinane skeleton.

## KEYWORDS

$\beta$ -Hydroxyalkylphosphine oxides / Phosphoric acid / Cyclization / Mechanism / DFT

## 1. Introduction

The intramolecular electrophilic substitution reaction is an operationally simple method for the synthesis of fused systems incorporating both aryl and cycloalkyl moieties.<sup>1</sup> Depending on the structure of the substrate different final structures including bicyclic,<sup>2</sup> tricyclic,<sup>3</sup> polycyclic<sup>4</sup> or spirocyclic<sup>5</sup> compounds could be obtained. Compounds with functional groups in the carbon skeleton may undergo cyclization to the corresponding fused systems with preservation of these

functionalities.<sup>6</sup> Some naturally occurring compounds have been synthesized using this reaction as one of the steps (Figure 1).<sup>7</sup>

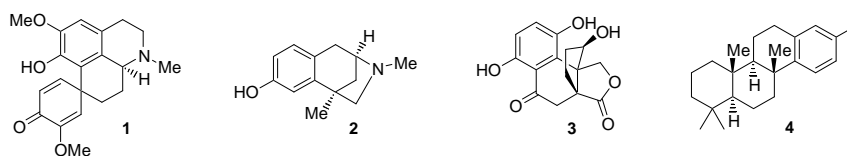
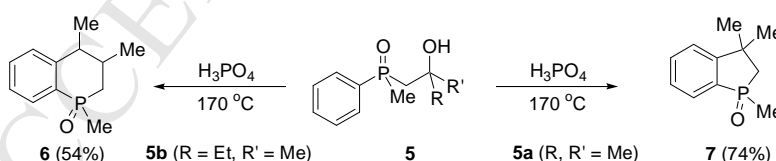


Figure 1. Examples of compounds synthesized using intramolecular cationic cyclization.

In organophosphorus chemistry, this reaction has found little applications so far. Only a few examples of intramolecular cyclization of alkenylphosphine oxides under acidic conditions or in the presence of a Lewis acid have been presented in the literature.<sup>8</sup> In this case, formation of either phosphaindane or benzophosphorinane oxides has been observed and the outcome of the reaction was dependent on the structure of alkenyl fragment. Apart from alkenylphosphine oxides, there are only two mentions regarding the cyclization of other precursors, namely  $\beta$ -hydroxyalkylphosphine oxides, under acidic conditions.<sup>9</sup> There was a suggestion that cyclization of these compounds might proceed either through preliminary dehydration to an alkene or through the direct formation of a carbocation but no evidence has been given to support any of these theories. Regarding the utility of this reaction as a tool in the formation of fused bicyclic systems it would be desirable to study in detail the mechanism of this transformation, especially in the cases where the rearrangement of the tertiary carbocation to the less stable secondary carbocation takes place prior to the cyclization step.

## 2. Results and discussion

In our previous paper,<sup>10</sup> we have described the intramolecular cyclization of  $\beta$ -hydroxyalkylphosphine oxides under acidic conditions (Scheme 1).

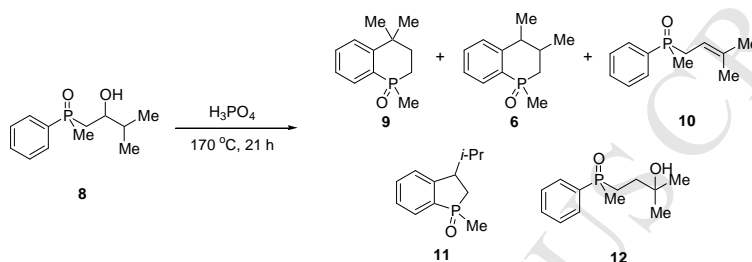


Scheme 1. Cyclization of **5a** and **5b** under acidic conditions.

Depending on the used substrate, either phosphaindane oxide **7** or benzophosphorinane oxide **6** could be obtained. The formation of **6** would require the prior rearrangement of the tertiary carbocation, obtained by OH-group removal under acidic conditions from the starting **5**, to the corresponding secondary carbocation. In general, selectivity of the reaction was strongly shifted towards the formation of fused 6,6-system (**6**) unless the primary carbocation had no possibilities to undergo rearrangement due to, for example, the length of the alkyl substituent at the carbinolic atom

like in **5a**. So far, the factors governing cyclization are not clear and it was therefore decided to perform more detailed studies to gain an insight into the mechanism of this reaction.

For test reactions, diastereomeric mixture of phenylmethyl(2-hydroxy-3-methylbutyl)-phosphine oxide **8** has been used as a model compound. We have already established that this product undergoes predominant cyclization towards benzophosphorinane.<sup>10</sup> What is more important, the product contains only one stereogenic center at the phosphorus atom which simplifies the analysis of the reaction mixture. At first, the correlation between the concentration of phosphoric acid and the selectivity of the reaction was verified (Scheme 2, Table 1).



Scheme 2. Influence of the concentration of phosphoric acid on the cyclization of **8**.

Table 1. Influence of the concentration of phosphoric acid on the cyclization of **8**.

Entry	$\text{H}_3\text{PO}_4$ concentration <sup>a</sup>	Products (%) <sup>b,c</sup>		
		<b>9</b>	<b>6</b>	<b>10/11/12</b>
1	99%	67	28	-/3/-
2	85%	83 (68)	17 (12)	-/-/-
3	73%	90 (68)	10 (6)	-/-/-
4	64%	92 (85)	8 (8)	-/-/-
5	57%	92 (90)	8 (8)	-/-/-
6	52%	2	-	3/-/27
7	35%	No reaction		

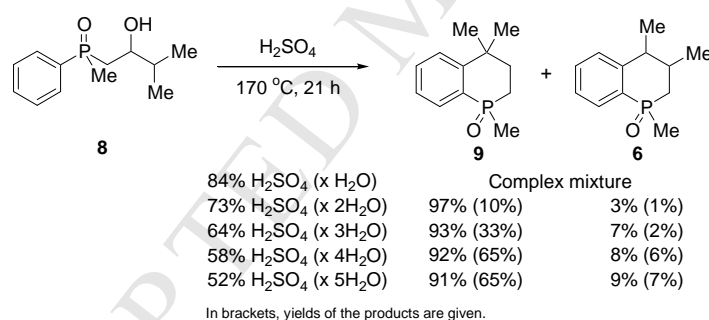
<sup>[a]</sup> 85% ( $\text{H}_3\text{PO}_4 \times \text{H}_2\text{O}$ ); 73% ( $\text{H}_3\text{PO}_4 \times 2\text{H}_2\text{O}$ ); 64% ( $\text{H}_3\text{PO}_4 \times 3\text{H}_2\text{O}$ ); 57% ( $\text{H}_3\text{PO}_4 \times 4\text{H}_2\text{O}$ ); 52% ( $\text{H}_3\text{PO}_4 \times 5\text{H}_2\text{O}$ ); 35% ( $\text{H}_3\text{PO}_4 \times 10\text{H}_2\text{O}$ ).

<sup>[b]</sup> Conversion based on  $^{31}\text{P}$  NMR analysis. <sup>[c]</sup> In brackets, isolated yields are given.

For these reactions, a huge excess of phosphoric acid has been used in order to assure the high concentration of  $\text{H}^+$  ions, i.e., phosphoric acid has been used as a solvent with a specific dielectric constant. Concentration of phosphoric acid used in the cyclization reaction has been adjusted to a formal hydration level of  $\text{H}_3\text{PO}_4$  molecule. To achieve the high selectivity of the reaction towards cyclization, high temperature must be applied, otherwise dehydration is the major reaction.<sup>10</sup> Thus,

the use of anhydrous phosphoric acid led to the formation of **9** as the major compound accompanied by some isomeric product **6**. The latter compound is formed from the isomeric secondary carbocation obtained by methyl group shift in the parent carbocation. The amount of this product depended strongly on the concentration of phosphoric acid. The use of aqueous phosphoric acid led to a decrease in the amount of this product down to 8% in 64%  $\text{H}_3\text{PO}_4$ . On the other hand, the formation of **9** increased with the decrease of  $\text{H}_3\text{PO}_4$  concentration and varied at 80-90% level in a wide concentration range (57-85%  $\text{H}_3\text{PO}_4$ ). The use of 52%  $\text{H}_3\text{PO}_4$  ( $\text{H}_3\text{PO}_4 \cdot 5\text{H}_2\text{O}$ ) led to a dramatic drop in the conversion towards **9** (Table I, Entry 6). In this reaction, the main product was **12**, the OH-group migration product along with many other unidentified species and unreacted substrate which was the main component of the mixture. Formation of this compound must involve dehydration of **8**, cation rearrangement followed by its reaction with water instead of cyclization.

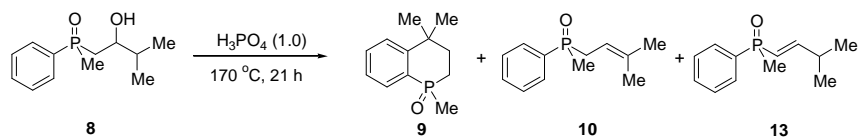
According to the data presented above, cyclization of compound **8** towards **9** effectively proceeds at relatively high  $\text{H}_3\text{PO}_4$  concentrations. This might cause problems during a work-up of the reaction mixture, especially when the whole amount of acid has to be neutralized. It was assumed that the use of stronger acid could result in a more effective transformation of the substrate, and therefore, allow a decrease in the amount of acid used. It was decided therefore to perform a set of the reactions in  $\text{H}_2\text{SO}_4$  and compare the results with those obtained using phosphoric acid (Scheme 3).



Scheme 3. Cyclization of **8** in  $\text{H}_2\text{SO}_4$ .

The concentration of sulfuric acid has been adjusted to the hydration level, similarly to phosphoric acid. Attempted cyclization in 84%  $\text{H}_2\text{SO}_4$  ( $\text{H}_2\text{SO}_4\text{-H}_2\text{O}$ ) led to the formation of a complex reaction mixture whereas dilution of sulfuric acid with water resulted in a dramatic increase of the reaction selectivity towards the cyclization pathway. It is possible that under strongly acidic conditions the substrate undergoes extensive decomposition in the presence of sulfuric acid which is not the case for more diluted solutions. The higher activity of sulfuric acid is evident when comparing the cyclization of **8** in media with lower acid concentration. With 52%  $\text{H}_3\text{PO}_4$ , the conversion of **8** towards **9** was only 2% whereas in 52%  $\text{H}_2\text{SO}_4$  it still reached 100%.

In another set of reactions, compound **8** has been treated with an equimolar amount of phosphoric acid but at different concentrations (Scheme 4, Table 2).

Scheme 4. Attempted cyclization with equimolar amount of  $\text{H}_3\text{PO}_4$  at different concentrations.Table 2. Attempted cyclization with equimolar amount of  $\text{H}_3\text{PO}_4$  at different concentrations.

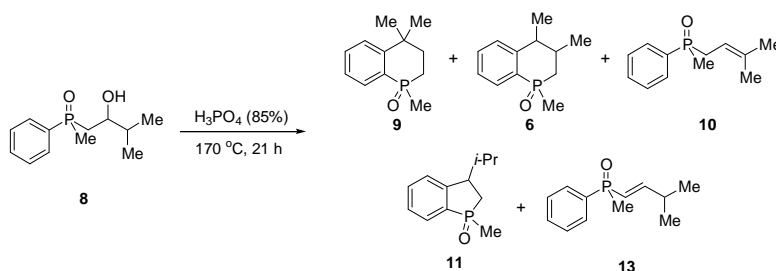
Entry	$\text{H}_3\text{PO}_4$ concentration <sup>a</sup>	Products <sup>b</sup>		
		<b>9</b>	<b>10</b>	<b>13</b>
1	99%	-	58%	5%
2	85%	1%	74%	7%
3	73%	1%	58%	6%
4	64%	3%	51%	4%
5	57%	1%	67%	5%
6	52%	-	75%	5%
7	35%	-	61%	4%

<sup>[a]</sup> 85% ( $\text{H}_3\text{PO}_4 \times \text{H}_2\text{O}$ ); 73% ( $\text{H}_3\text{PO}_4 \times 2\text{H}_2\text{O}$ ); 64% ( $\text{H}_3\text{PO}_4 \times 3\text{H}_2\text{O}$ ); 57% ( $\text{H}_3\text{PO}_4 \times 4\text{H}_2\text{O}$ ); 52% ( $\text{H}_3\text{PO}_4 \times 5\text{H}_2\text{O}$ ); 35% ( $\text{H}_3\text{PO}_4 \times 10\text{H}_2\text{O}$ ).

<sup>[b]</sup> Conversion based on  $^{31}\text{P}$  NMR analysis.

The most striking observation was the formation of  $\beta,\gamma$ -alkenylphosphine oxide **10** as the main and  $\alpha,\beta$ -alkenylphosphine oxide **13** as the minor reaction products. The formation of benzophosphorinanone oxide **9** is extremely strongly inhibited, irrespectively of the concentration of the used phosphoric acid. It appeared that the selectivity of this reaction is dependent on the amount of acid and can be shifted from dehydration to cyclization.

Therefore, it was decided to find out the relation between the amount of an acid and the selectivity of the reaction (Scheme 5, Table 3). The data collected in Table 3 show a clear correlation between the reactivity of substrate and the amount of acid used. With 0.5 equiv. of 85%  $\text{H}_3\text{PO}_4$  the only products were alkenylphosphine oxides **10** and **13** (Table 3, Entry 1). However, with 2 equiv. of acid the formation of reasonable amounts of cyclization product **9** has been observed although the selectivity was low due to the formation of side products (see also Supporting Information). A detailed analysis of this mixture using  $^{31}\text{P}$  NMR technique suggested that some signals might correspond to the isomeric products with shifted OH-group.



Scheme 5. Influence of the amount of acid on the selectivity of the reaction.

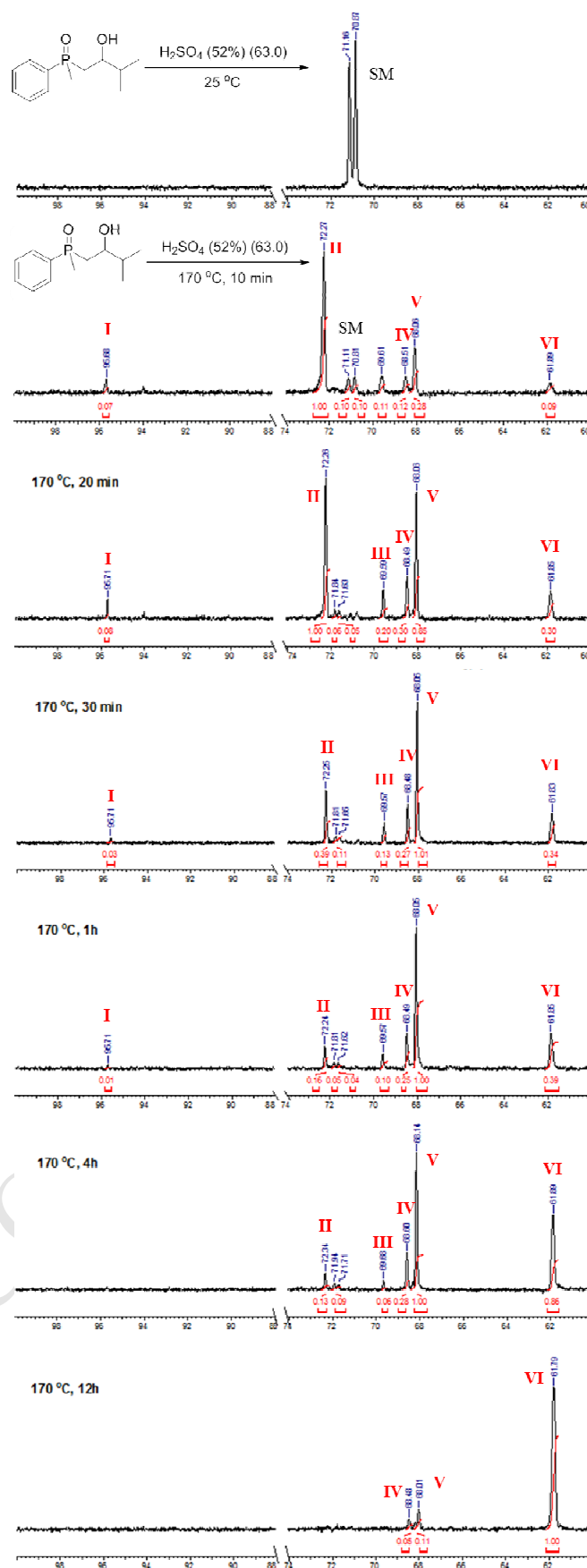
Table 3. Influence of the amount of acid on the selectivity of the reaction.

Entry	Acid (equiv.)	Products (%) <sup>a</sup>				
		<b>9</b>	<b>6</b>	<b>10</b>	<b>11</b>	<b>13</b>
1	0.5	-	-	52	-	48
2	1	1	-	74	-	7
3	2	20	3	22	-	1
4	3	67	20	-	1	-
5	4	64	13	-	1	-
6	5	64	15	-	8	-
7	10	77	17	-	6	-
8	20	82	17	-	1	-
9	50	85	14	-	1	-

<sup>[a]</sup> Conversions based on NMR analysis.

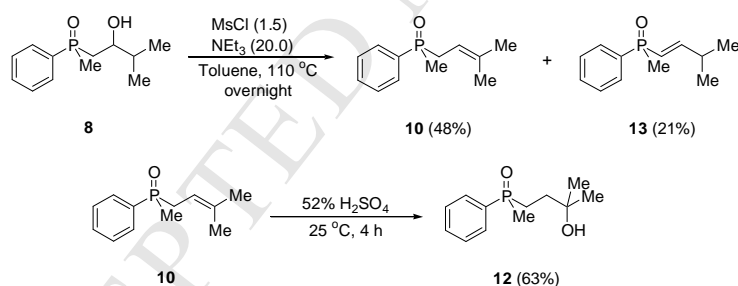
Selectivity of the tested reaction appeared to increase with the increase of the amount of phosphoric acid. The use of 5 equiv. of  $\text{H}_3\text{PO}_4$  was found to be enough for the selective cyclization and only trace amounts of other products were observed in the reaction mixture. Further increase of the amount of acid still increased the selectivity towards cyclic products but to a much lesser degree.

The experiments conducted so far were mostly directed towards the optimization of the reaction conditions in order to achieve the best selectivity towards bicyclic product. For organophosphorus compounds,  $^{31}\text{P}$  NMR spectroscopy is an ideal tool to follow the reaction course but in this case this method is completely useless due to the presence of a large excess of phosphoric acid in the mixture. Luckily, sulfuric acid appeared to be a good substitute to phosphoric acid. Therefore, cyclization of **8** in 52% sulfuric acid has been followed by  $^{31}\text{P}$  NMR. The mixture was heated for a specified time, then cooled to rt and analyzed by NMR technique. The outcome is presented in Figure 2.

Figure 2. Conversion of **8** with time followed by  $^{31}\text{P}$  NMR.

First, NMR analysis of the solution of **8** in 52% H<sub>2</sub>SO<sub>4</sub> has been performed, which revealed the presence of two peaks at 71.16 ppm and 70.87 ppm, respectively, corresponding most probably to both diastereomers of protonated **8**. Analysis of the reaction mixture heated at 170 °C for 10 min showed the excessive transformation of the substrate. <sup>31</sup>P NMR spectra pointed out the presence of only traces of substrate, whereas the main single peak appeared at 72.27 ppm. The other peaks were at 96.68, 69.61, 68.51, 68.06 and 61.89 ppm, respectively. Heating the mixture for a longer time revealed further changes. The low intensity peak **I** at 96.68 ppm decreased slowly and disappeared completely after 4 h. The peak **II** at 72.27 ppm appeared as major product after heating for 10 min, decreased slowly and disappeared after 12 h. Peaks **III** and **IV** at 69.61 and 68.51 ppm, respectively, appeared after heating the tube for 10 min and decreased slowly during 12 h. Peak **V** at 68.06 ppm appeared after heating the mixture for 10 min, became the major after 30 min of heating and almost vanished after 12 h. Finally, very low intensity peak **VI** at 61.89 ppm appeared after 10 min of heating. Upon further heating, this peak became almost the sole one after 12 h.

At this moment it was clear that the transformation of **8** under acidic conditions proceeds with the formation of several intermediate compounds of yet unknown structure. It was assumed that the intermediate compounds might be alkenylphosphine oxides **10** and **13** or isomerized hydroxyalkylphosphine oxide **12**. Each of them has been prepared independently (Scheme 6) and then mixed with 52% H<sub>2</sub>SO<sub>4</sub> (Figure 3).



Scheme 6. Synthesis of **10**, **12** and **13**.

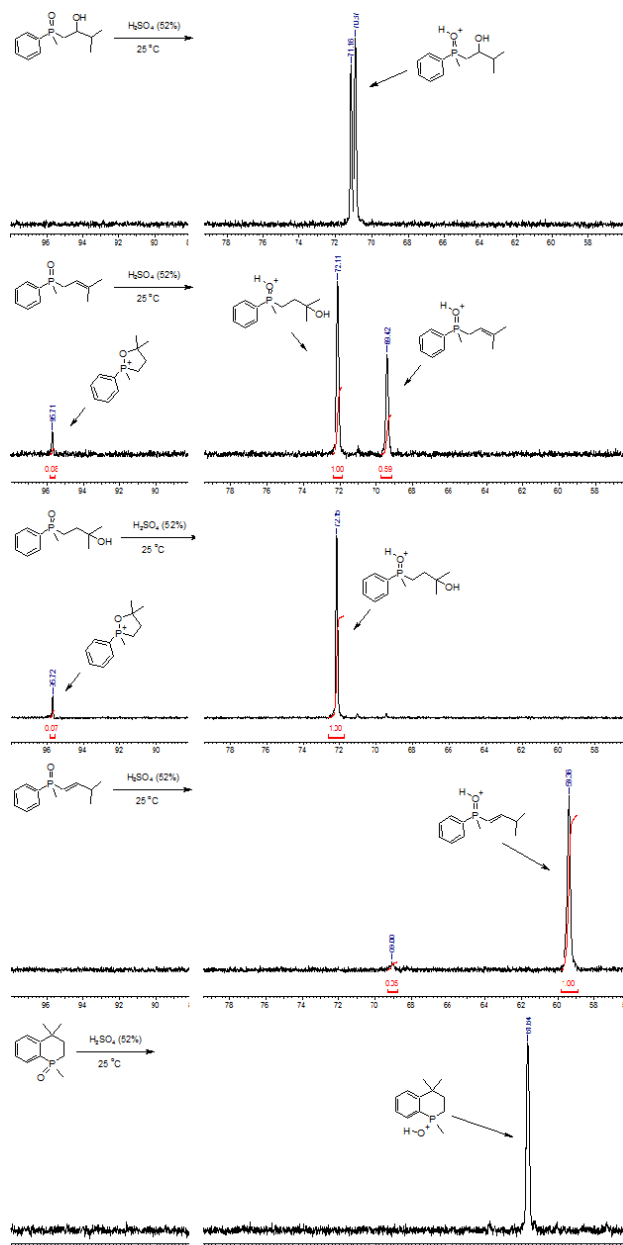


Figure 3.  $^{31}\text{P}$  NMR shifts of **8**, **9**, **10**, **12** and **13** in 52%  $\text{H}_2\text{SO}_4$ .

$^{31}\text{P}$  NMR analysis of **12** in sulfuric acid revealed the presence of two peaks. The first at 72.15 ppm corresponds to the protonated **12** whereas the peak at 95.72 ppm is most probably the cyclic oxaphospholanium cation, which is in accordance with literature data.<sup>11</sup> NMR analysis of alkenylphosphine oxide **10** in 52%  $\text{H}_2\text{SO}_4$  revealed the presence of three peaks, at 95.71, 72.11 and 69.42 ppm, respectively. Peaks at 95.71 ppm and 72.11 ppm correspond to cyclic oxaphospholanium cation and protonated  $\gamma$ -hydroxyalkylphosphine oxide **12**, respectively, and the last peak must therefore correspond to the protonated alkenylphosphine oxide **10**. It became clear from these spectra that phosphine oxide **10** exhibits high reactivity under acidic conditions and quickly undergoes formal water addition, most probably through the intermediate oxaphospholanium cation.  $^{31}\text{P}$  NMR analysis

of alkenylphosphine oxide **13** in 52%  $\text{H}_2\text{SO}_4$  revealed the presence of only one peak at 59.36 ppm whereas benzophosphorinane oxide **9** mixed with sulfuric acid afforded only one peak at 61.64 ppm.

$^{31}\text{P}$  NMR shifts of potential intermediates shown in Figure 3 enable preliminary mechanism for the transformation of **8** into **9** to be proposed. It seems that the first step is the formal OH-group migration. Regarding the presence of oxaphospholanium cation **I** in the mixture, this process is most likely to proceed through  $\text{H}^+$ -catalyzed intramolecular oxygen addition to C=C bond by phosphoryl oxygen as internal nucleophile and subsequent hydrolysis of oxaphospholanium cation. The second step is most probably protonation of the isomerized  $\gamma$ -hydroxyalkylphosphine oxide **12** (peak **II**) which in turn might undergo either water elimination and formation of alkenylphosphine oxide **10** (peak **III**) or cyclization to fused system **9** (peak **VI**). The presence of small amounts of alkenylphosphine oxide **10** (peak **III**) in the reaction mixture reflects its instability under the acidic conditions shown above. Peaks **IV** and **V** at 68.49 and 68.06 ppm, respectively, must therefore belong to the unknown intermediates. It is evident, however, that they undergo transformation into the final bicyclic products as can be judged from  $^{31}\text{P}$  NMR analysis.

Experimental data collected so far give some ideas about the mechanism of this reaction but some questions could not be answered solely using experimental techniques. It was therefore decided to apply computational methods to the analyzed reaction. First, the choice of the model substrate should be considered. The use of oxide **8** would not be the best option as in this case the formation of phosphaindane skeleton is *a priori* excluded. It was therefore decided to use phosphine oxide **5b** for DFT calculations as in this case the selectivity of the formation of either phosphaindane or benzophosphorinane oxides could be discussed. In the case of **5b** four isomers should be considered due to the presence of two stereogenic centers in the molecule. However, it was decided to use only the diastereomer possessing  $R_P$  configuration at phosphorus through all simulation steps for practical reasons.

Our main results were obtained with the aid of the density functional theory (DFT) approach.<sup>12</sup> In all reported cases the B3LYP hybrid functional<sup>13</sup> in conjunction with the polarized valence triple zeta (VDZP) basis set 6-311++G\*\*<sup>14</sup> was used. B3LYP is known to predict very accurate molecular geometries and energetics; in fact, it is one of the most accurate functionals and definitely the most frequently used at present. Due to the fact that some of the investigated systems were transition states, in which distances between the fragments of interest were of the order of 2 Å, the additional inclusion of the diffuse functions (++) is desirable. The calculations were carried out using the PQS quantum chemistry package.<sup>15</sup> Default geometry convergence criteria were adopted. However, thresholds for the integral prescreening in the SCF, gradient and hessian routines were preset to be two orders of magnitude lower than the default values. As the reactions are carried out in solution the solvent effect should have, in principle, been modeled. However, the intermolecular interactions in strongly acidic conditions are mostly of the hydrogen bonding type (the so-called specific interactions) and therefore the most commonly used conductor-like screening model (COSMO)<sup>16</sup> cannot be reliably applied.

Therefore, whenever necessary, those specific interactions were accounted for by attaching/detaching, e.g.,  $\text{H}_3\text{O}^+$  to the relevant molecule/intermediate (the so-called explicit solvation model, ESM). Besides, we did some tests using COSMO model with the dielectric constant characteristic of the solvent. The relative energies and energy barriers were affected to minor extent, insignificant for the final conclusions.

The geometry optimization for all the systems considered in this work followed by the frequency calculations were performed. Type of the obtained stationary point was determined based on the analysis of the vibrational frequencies. In the case of minima all computed frequencies were real. On the other hand one imaginary frequency was obtained in the case of each transition state. Visual inspection of the corresponding eigenmode allowed us to recognize species on each side of a transition state. The obtained energies were then used to calculate energy changes and barriers. All the reported energies were corrected for the zero point vibrational energies (ZPVE). In the case of the rearrangement (e.g., alkyl or hydride migration) or cyclization processes which are the most important steps in the overall mechanism ZPVE is usually (well) below 1 kcal/mol and therefore it is not essential in our considerations. In the case of processes accompanied by the change of a number of vibrational degrees of freedom (e.g., water association/dissociation) it was often found to be as large as ca. 2 kcal/mol. Therefore the overall discussion will be based on the ZPE-corrected values.

It was clear, that cyclization must occur through the formation of the intermediate tertiary carbocation from the parent **5b**. The protonation mechanism of **5b** has been considered which led to the conclusion that the initial  $\text{H}_3\text{O}^+$  attack occurs rather at phosphoryl oxygen and the obtained cation might undergo either water molecule removal affording cation **14** or addition of another  $\text{H}^+$  species leading to the corresponding dication (see Figure 3 (species IV-VI) in Supporting Information).

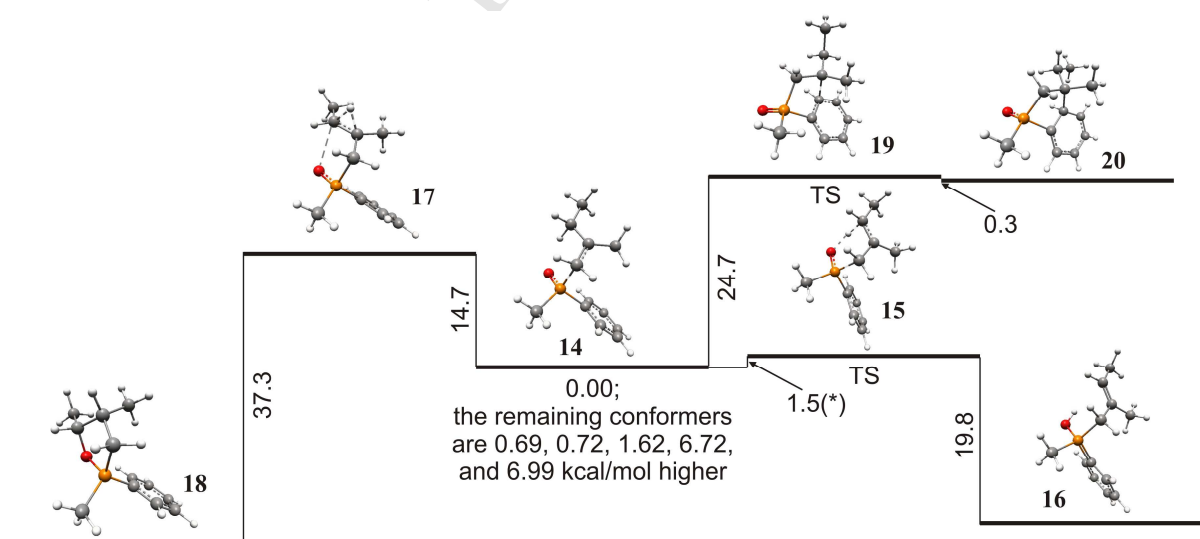


Figure 4. Possible transformations of **14** according to DFT calculations. Values next to the vertical lines refer to energy differences (in kcal/mol). (\*) ZPVE-uncorrected value.

The calculations performed for the cation **14** revealed the presence of several stable conformers. Therefore further calculations were run starting from the most stable one, as depicted in Figure 4, with torsion angle between cationic carbon atom and phosphoryl oxygen being  $-43^\circ$ , i.e., the cationic carbon atom is placed inbetween oxygen and phenyl. Its conversion into one of the diastereomeric bicyclic cyclization products **20** (with the *ipso* hydrogen atom and phosphoryl oxygen in *cis* arrangement) could be achieved through the transition state **19** which is 24.7 kcal/mol above than the parent cation. Structural change in the parent carbocation **14** approaching the transition state **19** is associated with change of the torsion angle between phenyl group and cationic carbon atom, i.e., this carbon atom should reorient towards one of the *ortho* positions in phenyl substituent.

The structure of the transition state **19** obtained by molecular modeling is close to the structure of the cyclic product **20** which suggests a quite small difference in the stability of these two species. Indeed, the gain of energy passing from the transition state to **20** is only 0.3 kcal/mol. Overall, the cyclization process appears to be endothermic – **20** is less stable than the parent tertiary carbocation by *ca.* 24.4 kcal/mol. It should be pointed out, that the cyclization of **14** depicted in Figure 4 represents only the most obvious possibility due to the proximity of the reacting centers. Also, reaction between cationic carbon atom and distant *ortho* position should be considered once **14** undergoes a slight conformational change (change of the  $C^+-C-P-O$  torsion angle). This leads to a different transition state with *ipso* hydrogen and phosphoryl oxygen being in *trans* arrangement (figure not shown). It appeared that the activation energy needed to reach an alternative transition state is lower than that depicted in Figure 4 (23.8 kcal/mol) along with the higher energy gain after the formation of internal carbon-carbon bond (3.1 kcal/mol).

Attempted calculations of the benzophosphorinanone pathway led to quite interesting results (Figure 4). Despite numerous attempts, only one stable secondary carbocation has been found, about 19 kcal/mol less stable than the parent **14** (not shown). Unfortunately, it was not possible to find the appropriate transition state for the cation rearrangement. Instead, hydride migration seems to induce the formation of pentacyclic oxaphospholanium cation **18** through the transition state **17**. Further transformation of these species would probably lead to the formation of isomeric  $\gamma$ -hydroxyalkylphosphine oxide after a reaction with water. This process, by the way, might be responsible for the formation of alcohol **12** in the reaction of **8** with 52%  $H_3PO_4$  or even isomeric alcohols observed in our previous work.<sup>10</sup>

The energy needed to reach the transition state **17** from **14** was found to be 14.7 kcal/mol which is 10 kcal/mol less than the energy needed to reach the transition state **19**. Moreover, energy released by passing from **17** to **18** was far higher (37.3 kcal/mol) than the energy released in the formation of cyclization product **20** (0.3 kcal/mol). Regarding that, it is unlikely for cation **14** to undergo cyclization towards bicyclic benzophosphorinanone and phosphaindane frameworks.

The structural analysis of cation **14** also revealed that there might be a quite easy proton shift between the  $\gamma$  carbon atom and phosphoryl oxygen (Figure 4). A search for the transition state

revealed that there is only slight rise in energy between **14** and transition state **15** (1.5 kcal/mol). This value, however, is uncorrected for ZPVE as the attempted correction of the energy led to the transition state slightly lower in energy than the starting **14**. Such a result is a consequence of the approximate character of the calculations which lead to inaccuracies in the calculated uncorrected relative energies. In particular, the order of species may be altered upon adding ZPVE for small activation energies.

The transformation of cation **14** through the transition state **15** leads to protonated alkenylphosphine oxide **16** with release of energy (19.8 kcal/mol). Overall, the formed product is 18.3 kcal/mol more stable than the parent **14**. Due to a low activation barrier this pathway seems to be kinetically favorable for the transformation of  $\beta$ -hydroxyalkylphosphine oxide **8** in the presence of small amounts of acid. This was actually observed in the case where a stoichiometric amount of acid has been used (see Table 2). It was therefore interesting to find, whether **16** might be reactivated for the cyclization reaction (Figure 5).

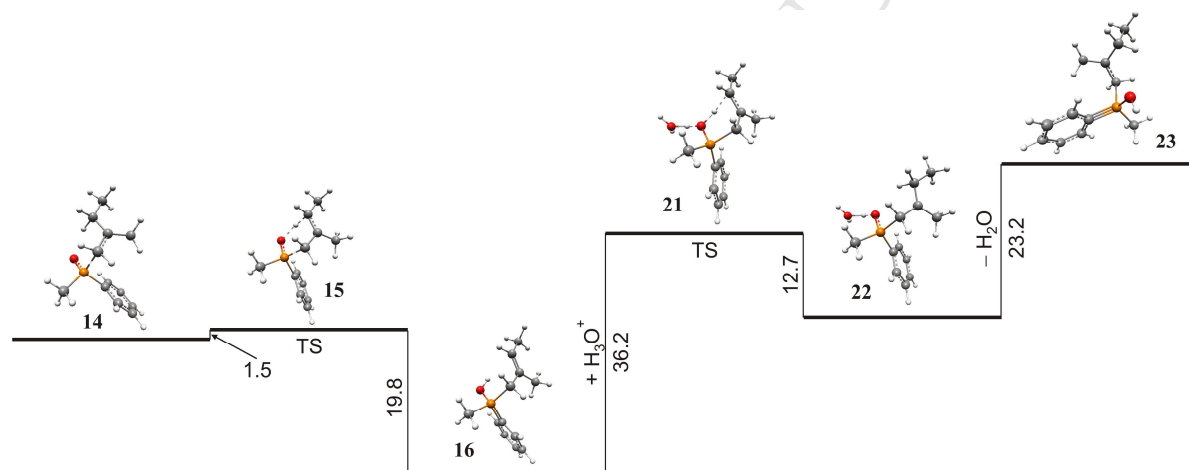


Figure 5. Protonation of **16**. Values next to the vertical lines refer to energy differences (in kcal/mol).

Two potential  $\text{H}_3\text{O}^+$  approaches to **16** should be considered. The first is the attack of  $\text{H}_3\text{O}^+$  at the phosphoryl oxygen with the consecutive proton shift from oxygen to the  $\gamma$  carbon atom or the direct attack of  $\text{H}_3\text{O}^+$  cation on C=C bond. Both approaches have been considered and the first one appeared to be slightly more favorable (by 1.5 kcal/mol). This reaction proceeds through the transition state **21** and is quite energy-consuming (36.2 kcal/mol). The transformation of **21** into the tertiary carbocation **22** appears to proceed with a slight stabilization of the molecule (12.7 kcal/mol). The possible transformation of these species could involve  $\text{H}_3\text{O}^+$  dissociation which should lead to the formation of **14** or dissociation of  $\text{H}_2\text{O}$  molecule which would afford dication **23** (23.2 kcal/mol less stable than **22**).

As follows from DFT calculations the cation **14**, the most obvious candidate for cyclization, undergoes rather C=C or C-O bond formation instead of cyclization. Therefore, it must be the dication **23** that follows the pathway leading to cyclic products. It is essential to use at least two equivalents of acid to ensure the presence of an appropriate amount of  $\text{H}_3\text{O}^+$  species which should lead to the

dication. It is also clear now, that the use of an equimolar amount of acid inevitably leads to the formation of elimination products as there is simply not enough acid to form the dication in a reasonable timescale, all the more that the formation of **23** is a non-favorable process compared to the formation of **14**. The calculations show also, that the formation of alkenylphosphine oxides like **16** might be the first process in the cyclization pathway. This process competes with the formation of cyclic oxaphosphonium species **18**, which probably leads to the formation of isomeric  $\gamma$ -hydroxyalkylphosphine oxides. The formation of the latter has been observed for some  $\beta$ -hydroxyalkylphosphine oxides.<sup>10</sup>

Once it became clear that dication **23** is the crucial intermediate in the cyclization pathway, further DFT calculations have been directed towards elucidation of the cyclization mechanism. When considering the cyclization of the dication **23** it appears clear that, in fact, four transition states and four intermediate cyclic carbocations should be considered. This is the consequence of the two *ortho* positions present in phenyl substituent (Figure 6).

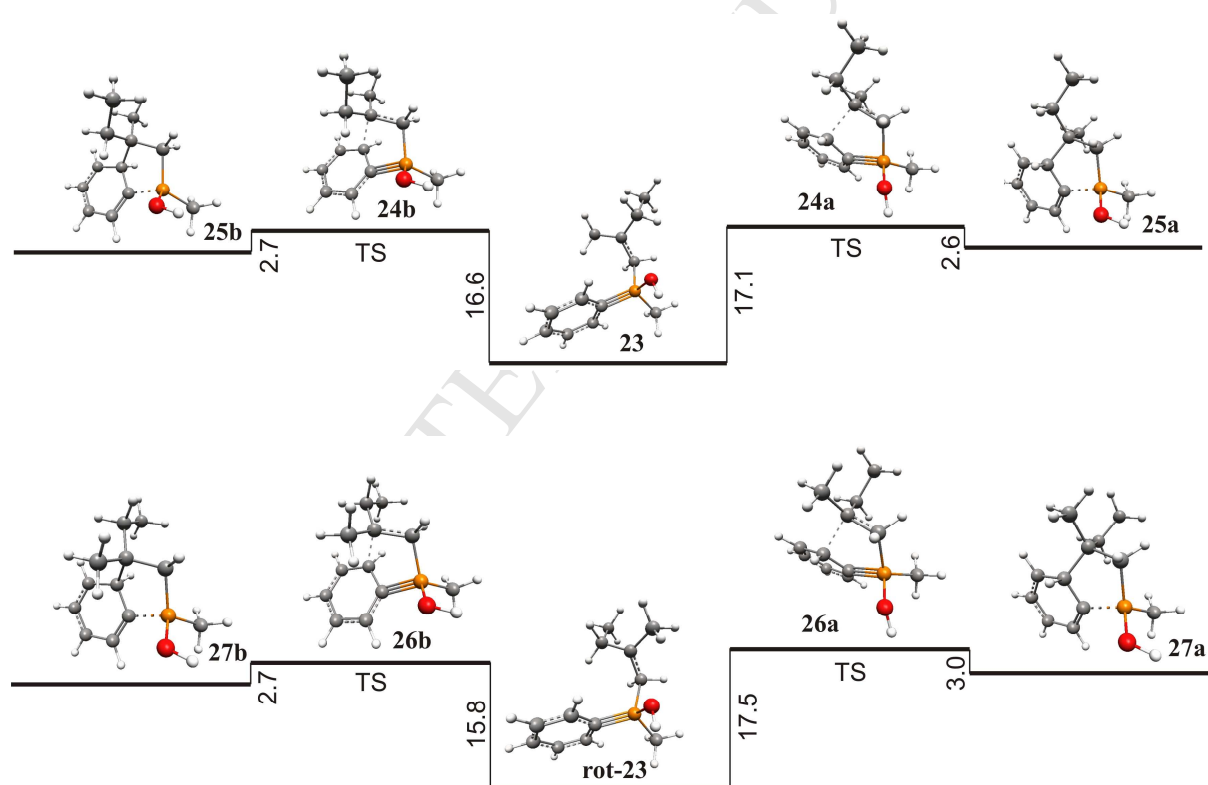


Figure 6. Cyclization of **23** and **rot-23** optimized by DFT calculations. Values next to the vertical lines refer to energy differences (in kcal/mol).

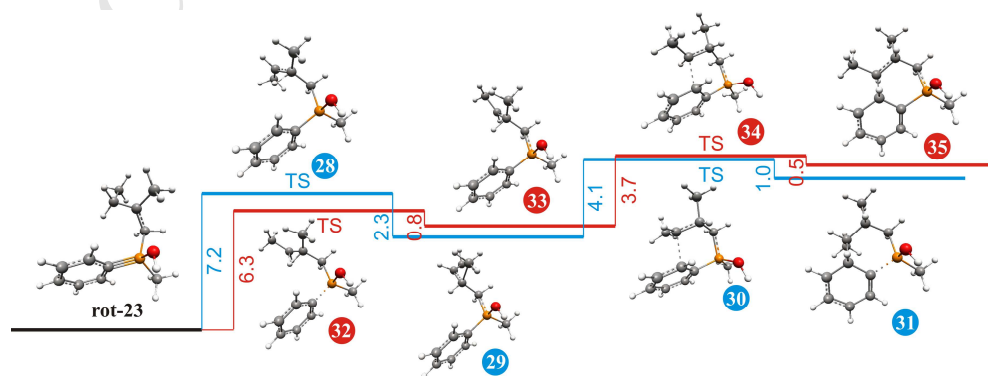
For dication **23**, it is possible to imagine the reaction between the cationic carbon atom and either the proximal or distant *ortho* carbon atom. In the first case, the formation of cyclic cation **25a** with *syn* arrangement of *ipso* hydrogen and phosphoryl oxygen, whereas in the second – **25b** with *anti*

arrangement should be expected (Figure 6). These two structures differ only in the absolute configuration at the former *ipso* carbon atom and, therefore, both will collapse into the same product upon rearomatization step. The same situation should appear for dication **rot-23**: two cyclic structures, **27a** and **27b** should be formed through transition states **26a** and **26b**, respectively. For all possible transition states the activation energy varies from 15.8 kcal/mol for **26b** to 17.5 kcal/mol for **26a**, i.e., there are only slight differences in energy barriers in the formation of phosphaindane core. Similarly, the energy gained during the formation of carbon-carbon bond lies in the range 2.6-3.0 kcal/mol. Structures of the obtained transition states and cyclic dications are similar which explains the minor energy release when passing from the transition state to the product.

Cyclization pathway analysis shows that the configuration of the newly formed chirality centre at the  $\beta$  carbon atom depends on the mutual arrangement of *ortho* carbon atom and tertiary cation. Depending on the face of carbocation approaching to the *ortho* carbon atom, either *R* or *S* configuration at the  $\beta$  carbon atom is possible. It is seen in Figure 6 that both approaches are equally probable. Moreover, the calculated energy scan with respect to the rotation around the  $C_\alpha$ - $C_\beta$  bond in the carbocation revealed only small rotational energy barrier (3.4 kcal/mol) (see Supporting Material) which suggests that there are no virtual restrictions for the mutual interconversion of both conformers.

The rearomatization mechanism with two possible pathways has also been studied (see Supporting Information). In the first approach, the rearomatization of the indane fragment was supposed to proceed first whereas in the second – the proton removal from phosphoryl oxygen was the first step. The DFT calculations strongly supports the mechanism where the rearomatization is the first process.

The experimental data obtained so far show a great selectivity in the formation of the benzophosphorinane systems, whenever the isomerization of the parent carbocation is possible. It was therefore decided to calculate cyclization of carbocation **rot-23** as a model intermediate towards fused 6,6 systems (Figure 7). The same analysis should be performed for dication **23** but it seems reasonable to conclude that the energy profile for transformation of this dication should be very similar and, therefore, DFT calculations were limited only to **rot-23**.



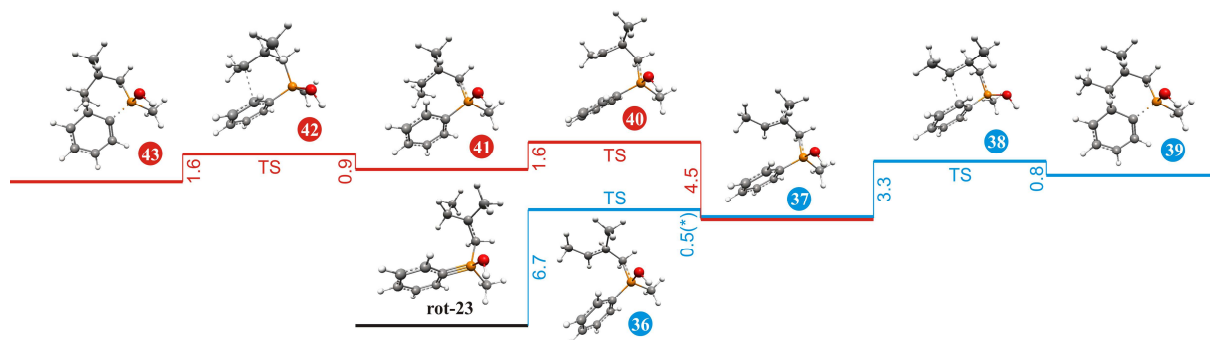


Figure 7. Cyclization of **rot-23** towards benzophosphorinane core optimized by DFT calculations. Values next to the vertical lines refer to energy differences (in kcal/mol). (\*) ZPVE-uncorrected value.

Cyclization of **rot-23** towards bicyclic benzophosphorinane core must include preliminary rearrangement of a tertiary carbocation to the corresponding secondary carbocation. Migration of hydride from the  $\gamma$  to  $\beta$  carbon atom will induce the formation of a new chirality centre at the  $\beta$  carbon atom. Due to the flat structure of the carbocation the absolute configuration of the newly formed chirality centre will depend only on the side of hydride migration. Moreover, the presence of two hydrogen atoms at  $\gamma$  carbon atom gives a possibility for different arrangement of two methyl groups during the rearrangement step.

It was therefore decided to investigate the rearrangement of **rot-23** into the secondary carbocation by hydride migration from the side *syn* to the phenyl group (Figure 7) which should lead to a new chirality centre at the  $\beta$  carbon atom with *R* configuration. Due to the presence of two  $\gamma$  hydrogen atoms two transition states **28** and **32** have been found which lead to the corresponding secondary carbocations **29** and **33**, respectively. Activation energies needed to achieve transition states were found to be 7.2 kcal/mol and 6.3 kcal/mol, respectively. Interestingly, the activation energy for hydride transfer is lower for *cis* orientation of two methyl groups than for *trans* orientation although the energy release when passing from **28/32** to **29/33** is higher for *trans* oriented carbocation (2.3 kcal/mol vs. 0.8 kcal/mol).

Carbocations **29** and **33** are formally rotamers with only slightly different energies which might suggest rather fluent mutual interconversion of these species through rotation about  $C_{\beta}-C_{\gamma}$  bond. Cyclization of these conformers leads to the formation of two different products **31** and **35** through transition states **30** and **34**, respectively, with either *S* (for **31**) or *R* (for **35**) configuration at the  $\gamma$  carbon atom. Analogously to cyclization of **23** and **rot-23** to phosphaindane core, an additional chirality centre at *ipso* carbon atom is formed which, in consequence, increases the number of the possible cyclic products. Since these chirality centers disappear during the rearomatization step, it was decided to omit the DFT calculations for these additional structures.

Regarding the favorable arrangement of the secondary carbocations **29** and **33**, their cyclization into benzophosphorinane skeleton requires far less energy for the activation compared to the energy

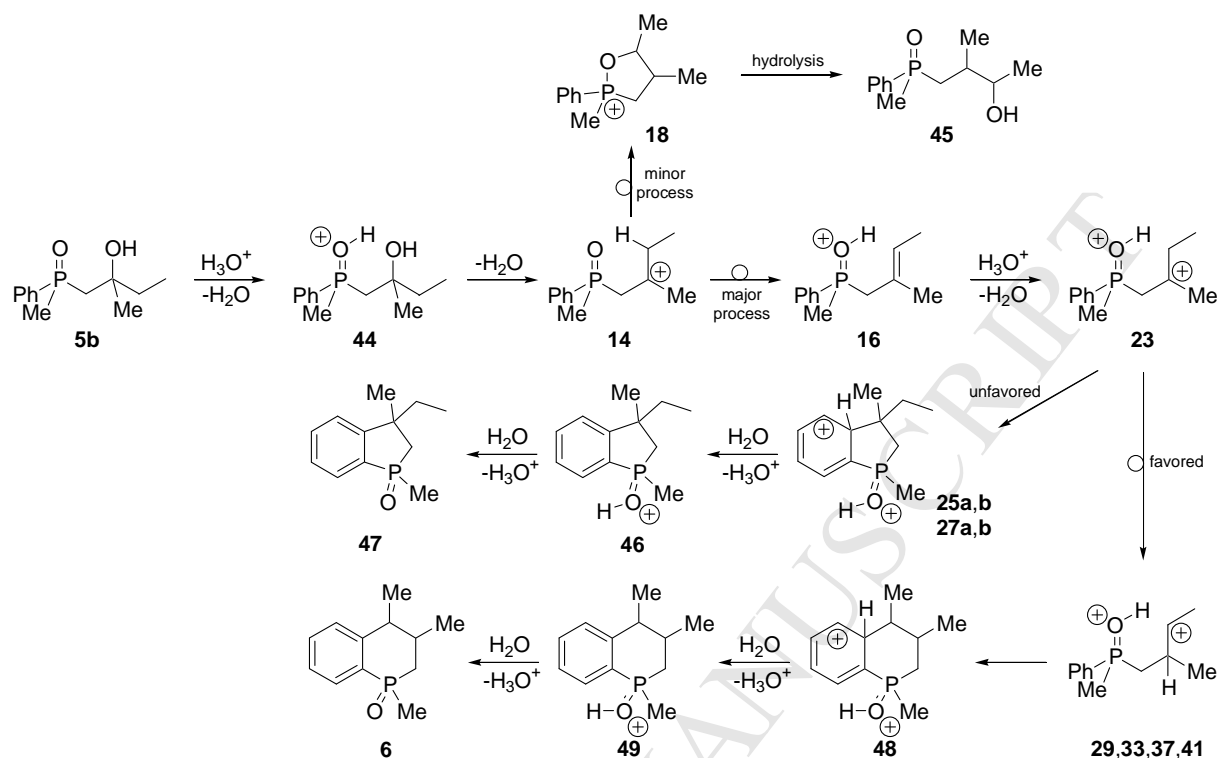
consumed in the cyclization towards phosphaindane. Thus, transition of the dication **29** to **31** requires only 4.1 kcal/mol to reach the transition state **30** which then collapses into **31** with but with only slight stabilization (1 kcal/mol). For transition of **33** to **35** these values are 3.7 kcal/mol and 0.5 kcal/mol, respectively. The values obtained for cyclization of the secondary carbocations suggest a very good steric adjustment of these species which facilitates cyclization step. The activation energy is most probably needed for slight conformational change of **29/33** to assure good overlapping of the orbitals.

In the next step, DFT calculations for hydride transfer in **rot-23** from the side *anti* to the phenyl group have been performed (Figure 7). This hydride shift should lead to formation of a new chirality centre at the  $\beta$  carbon atom with *S* configuration. Attempted calculations on cationic rearrangement led to only one intermediate **37** through a transition state **36** where two methyl groups were *cis*-arranged. Activation energy for this process was similar to the other two found previously (6.7 kcal/mol) whereas the stabilization energy was found to be only 0.5 kcal/mol. The latter value was not corrected for ZPVE for the reasons explained above. Cyclization of **37** is easily achieved with activation energy similar to the formation of **31** and **35** (3.3 kcal/mol).

The secondary cationic conformer analogous to **37** with *trans* arrangement of methyl groups could not be obtained starting from **rot-23** by a direct hydride transfer. Another possibility to obtain cation **41** is the rotation of  $\text{CH}_3\text{-CH}$  group around  $\text{C}_\beta\text{-C}_\gamma$  bond starting from **37** (Figure 7). This process appears to proceed through transition state **40** with an activation energy equal 4.5 kcal/mol and the conformer appeared to be slightly less stable than **37** (by 2.9 kcal/mol). Cyclization of **41** proceeds with very low activation energy (0.9 kcal/mol) and the cyclic product appeared to be more stable than the starting secondary cation.

An interesting conclusion can be drawn when comparing activation energies for cyclization of **23/rot-23** towards phosphaindane core **25a,b** and **27a,b** and cyclization towards benzophosphorinane core **31**, **35**, **39** and **43**. The activation energies for cyclization towards **25a,b** and **27a,b** (15.8-17.5 kcal/mol) are higher than the sum of energies needed to activate rearrangement-cyclization sequence towards **31**, **35**, **39** and **43** (9-10 kcal/mol). This means that cyclization of **23/rot-23** towards benzophosphorinane is kinetically favorable. DFT calculations for the final products revealed almost identical energy values for phosphaindane and benzophosphorinane oxides (see Supporting Information), therefore, the whole process seems to be driven by kinetic factors. It appeared also that hydride migration can proceed equally efficiently from both sides of planar  $\text{sp}^2$  carbon atom which makes this process completely non-stereoselective. Unrestricted rotation of terminal methyl group in secondary dications results in completely non-stereoselective formation of new chirality centers at the  $\gamma$  carbon atom in benzophosphorinane oxides. As a result, almost equimolar mixture of four benzophosphorinane oxides should be expected in the cyclization of **5b** which was confirmed experimentally.

Based on both experimental and computational data the overall acid-promoted cyclization of  $\beta$ -hydroxyalkylphosphine oxides proceeds as shown in the Scheme 7.



Scheme 7. The proposed mechanism for the acid-catalyzed cyclization of  $\beta$ -hydroxyalkylphosphine oxides.

The mechanism includes protonation of the starting **5b** which undergoes water removal and the formation of the tertiary carbocation **14**. Under the reaction conditions, this intermediate predominantly rearranges into protonated alkenylphosphine oxides **16** but also another type of rearrangement with the formation of cyclic oxaphospholanium cation **18** might take place to a limited extent. Its hydrolysis leads to  $\gamma$ -hydroxyalkylphosphine oxide **45**. Intermediate **16** undergoes protonation affording the dication **23** which then preferably undergoes proton shift and the formation of secondary carbocations **29**, **33**, **37** and **41** which in turn enter intramolecular cyclization with phenyl group at phosphorus affording upon work-up the final benzophosphorinane oxide **6**. The calculated sum of energies along the whole reaction pathway exactly matches the energy difference between the substrate and the product.

### 3. Conclusions

The main purpose of this research project was to discover the rules governing cyclization of  $\beta$ -hydroxyalkylphosphine oxides towards benzophosphorinane oxides and to understand the mechanism of this process, especially an unusual preference of these compounds to undergo cyclization towards benzophosphorinane oxides. It was found that concentration of an acid might have influenced the selectivity of the reaction. For phosphoric acid, the lowest

acceptable concentration for cyclization was found to be 57%, whereas for sulfuric acid even more diluted media still mediate effective cyclization. The use of equimolar amount of acid led only to dehydration of substrates. A detailed optimization of the reaction revealed that 3-fold excess of the acid is sufficient to promote effectively the cyclization of  $\beta$ -hydroxyalkylphosphine oxides. The transformation of **8**, followed by  $^{31}\text{P}$  NMR spectroscopy, revealed the fast rearrangement of substrate into the more substituted  $\gamma$ -hydroxyalkylphosphine oxide **12**, most probably through an intermediate formation of dehydration product and intramolecular cyclization catalyzed by the acid. DFT calculation performed on **5b** revealed that equimolar amount of acid leads mostly to dehydration of substrate, or to OH-group migration from  $\beta$  to  $\gamma$  carbon atom. In the presence of an excess of acid, protonation of phosphoryl oxygen is followed by OH-group protonation and subsequent water removal leading to tertiary dication. According to DFT calculations, activation energy needed for cyclization of this species towards phosphaindane core is higher than the sum of energies needed for cationic rearrangement and subsequent cyclization towards benzophosphorinane core. A comparison of relative energies of phosphaindane and benzophosphorinane oxides revealed almost equal stability of these compounds and, therefore, cyclization of  $\beta$ -hydroxyalkylphosphine oxides seems to be ruled by kinetic factors.

## 4. Experimental section

### 4.1. General information

All reactions were performed under an argon atmosphere using Schlenk techniques. Only dry solvents were used, and the glassware was heated under vacuum prior to use. Solvents for chromatography were distilled once before use, and solvents for extraction were used as received. Tetrahydrofuran was dried over sodium/benzophenone ketyl. *n*-BuLi was commercially available and used as received. *Analytics and Instruments.* The NMR spectra was recorded with Bruker Ascend (500 MHz) spectrometer in  $\text{CDCl}_3$  as a solvent at room temperature unless otherwise noted. Chemical shifts ( $\delta$ ) are reported in ppm relative to residual solvent peak and to internal ( $\text{H}_3\text{PO}_4$ ) standard in case of  $^{31}\text{P}$  NMR spectra. Mass spectra were recorded with Shimadzu GC-MS QP2010S spectrometer working in electron ionization (EI) mode with Phenomenex Zebron ZB-20HT INFERNO column using following parameters: pressure 65 kPa, total flow 33.9 mL/min, column flow 1.0 mL/min, linear velocity 36.8 cm/s, split 30, temperature program (80 °C hold 0.5 min, 80–300 °C/19 °C/min, hold 2 min, 300–340 °C/15 °C/min, hold 3.26 min, total ca. 20 min). Thin layer chromatography (TLC) was performed with precoated silica gel plates and visualized by UV light or iodide on silica gel. The reaction mixtures were purified by column chromatography over silica gel (60–240 mesh). Melting points were determined in a capillary tube.

4.2. (2-Hydroxy-3-methylbutyl)methylphenylphosphine oxide (**8**). In a flame-dried Schlenk tube (50 mL) equipped with magnetic stirrer and inert gas inlet was placed dimethylphenylphosphine oxide (0.326 g, 2.1 mmol) in THF (20 mL). The mixture was cooled to  $-78\text{ }^{\circ}\text{C}$  (dry ice-acetone) and *n*-BuLi (2.1 mmol, 1.6 M in hexane) was added. After the orange mixture was stirred for 50 min at  $-78\text{ }^{\circ}\text{C}$ , isobutyraldehyde (0.228 g, 3.17 mmol) was added until no colour remained. Reaction was allowed to warm to room temperature and was stirred for 1 hour. The reaction was quenched by addition of saturated  $\text{NH}_4\text{Cl}$  solution (10 mL) and extracted with DCM ( $3\times 20\text{ mL}$ ). The combined organic phases were dried over  $\text{MgSO}_4$ , filtered, and evaporated under reduced pressure. The residue was purified by flash column chromatography using hexane/ $\text{CHCl}_3$ /*i*-PrOH ( $v/v = 5:1:1$ ) as eluent yielding of two diastereomers 0.395 g, (83%), ( $dr = 52.5:47.5$ ).

*Major diastereomer*: Yield 45% (0.182 g, 38% isolated as a pure compound); white solid; mp  $90.3\text{--}92.1\text{ }^{\circ}\text{C}$ ;  $R_f = 0.52$  (Hexane/ $\text{CHCl}_3$ /*i*-PrOH 5:1:1); [Found: C, 63.89; H, 8.67.  $\text{C}_{12}\text{H}_{19}\text{O}_2\text{P}$  requires C, 63.70; H, 8.46%];  $\nu_{\text{max}}$  (ATR) 3236, 2948, 2910, 2866, 1436, 1382, 1326, 1286, 1221, 1169, 1114, 1093, 1036, 887, 694, 689, 553, 507, 477, 418;  $\delta_{\text{H}}$  (500 MHz,  $\text{CDCl}_3$ ) 0.86 (d,  $J = 6.6\text{ Hz}$ , 3H), 0.87 (d,  $J = 3.8\text{ Hz}$ , 6H), 1.59–1.70 (m, 1H), 1.78 (d,  $J = 13.6\text{ Hz}$ , 3H), 1.88–1.97 (m, 1H), 2.00–2.11 (m, 1H), 3.75–3.83 (m, 1H), 4.52 (bs, 1H), 7.43–7.53 (m, 3H), 7.66–7.73 (m, 2H);  $\delta_{\text{C}}$  (126 MHz,  $\text{CDCl}_3$ ) 17.3, 17.6 (d,  $J = 69.9\text{ Hz}$ ), 17.8, 34.6 (d,  $J = 11.8\text{ Hz}$ ), 34.9 (d,  $J = 70.8\text{ Hz}$ ), 70.8 (d,  $J = 5.4\text{ Hz}$ ), 128.6 (d,  $J = 11.8\text{ Hz}$ ), 129.7 (d,  $J = 9.1\text{ Hz}$ ), 131.6 (d,  $J = 2.7\text{ Hz}$ ), 133.5 (d,  $J = 96.3\text{ Hz}$ );  $\delta_{\text{P}}$  (202 MHz,  $\text{CDCl}_3$ ) 40.27; GC tR = 9.89 min; GC–MS (EI, 70 eV):  $m/z$  (%) = 208 ( $\text{M}^+ - \text{H}_2\text{O}$ ) (3), 183 (72), 154 (12), 140 (37), 139 (100), 125 (18), 91 (29), 77 (26), 47 (16).

*Minor diastereomer*: Yield 37% (0.140 g, 29% isolated as a pure compound); colorless oil;  $R_f = 0.42$  (Hexane/ $\text{CHCl}_3$ /*i*-PrOH 5:1:1); [Found: C 63.92; H 8.71.  $\text{C}_{12}\text{H}_{19}\text{O}_2\text{P}$  requires C 63.70; H 8.46%];  $\nu_{\text{max}}$  (ATR) 3308, 2969, 2902, 2859, 1437, 1359, 1291, 1237, 1158, 1118, 1071, 1019, 965, 890, 740, 693, 668, 519, 490, 460, 437;  $\delta_{\text{H}}$  (500 MHz,  $\text{CDCl}_3$ ) 0.90 (d,  $J = 6.9\text{ Hz}$ , 3H), 0.94 (d,  $J = 6.9\text{ Hz}$ , 6H), 1.69–1.76 (m, 1H), 1.78 (d, 3H,  $J = 12.9\text{ Hz}$ ), 1.94–2.12 (m, 2H), 3.87–3.96 (m, 1H), 4.06 (bs, 1H), 7.46–7.56 (m, 3H), 7.67–7.75 (m, 2H);  $\delta_{\text{C}}$  (126 MHz,  $\text{CDCl}_3$ ) 16.1 (d,  $J = 69.9\text{ Hz}$ ), 17.5, 17.9, 34.6 (d,  $J = 11.8\text{ Hz}$ ), 34.9 (d,  $J = 69.9\text{ Hz}$ ), 71.6 (d,  $J = 5.4\text{ Hz}$ ), 128.7 (d,  $J = 11.8\text{ Hz}$ ), 129.6 (d,  $J = 10.0\text{ Hz}$ ), 131.8 (d,  $J = 2.7\text{ Hz}$ ), 133.8 (d,  $J = 97.2\text{ Hz}$ );  $\delta_{\text{P}}$  (202 MHz,  $\text{CDCl}_3$ ) 40.14; GC tR = 10.04 min; GC–MS (EI, 70 eV):  $m/z$  (%) = 208 ( $\text{M}^+ - \text{H}_2\text{O}$ ) (4), 183 (75), 154 (12), 140 (32), 139 (100), 125 (14), 91 (28), 77 (23), 47 (14). Analytical data are in accordance with those reported in the literature.<sup>9</sup>

4.3. 1,4,4-Trimethyl-1,2,3,4-tetrahydrophosphinoline 1-oxide (**9**). (2-Hydroxy-3-methylbutyl)methylphenylphosphine oxide (**8**) (0.105 g, 0.46 mmol) was stirred at  $170\text{ }^{\circ}\text{C}$  with 57%  $\text{H}_3\text{PO}_4$  (2.803 g, 16.30 mmol) for 21 h. The mixture was cooled below  $100\text{ }^{\circ}\text{C}$  and poured on to ice-water (10 mL). The dark brown mixture was extracted with dichloromethane or chloroform (4 x 20 mL). The aqueous solution was washed with sodium hydrogen carbonate solution (10 mL) and water

(10 mL). The extracts were dried over  $\text{MgSO}_4$ , filtered, and evaporated under reduced pressure. The residue was purified by column chromatography using AcOEt /MeOH (v/v = 9:1) as eluent yielding a pale yellow oil; yield 0.095 g (90%, isolated as a mixture with 8% of **6**);  $R_f$  = 0.26 (AcOEt/MeOH 9:1);  $\delta_{\text{H}}$  (500 MHz,  $\text{CDCl}_3$ ) 1.31 (s, 3H), 1.32 (s, 3H), 1.65 (d,  $J$  = 12.6 Hz, 3H), 1.87 - 1.98 (m, 1H), 2.04 - 2.15 (m, 2H), 2.22 - 2.32 (m, 1H), 7.27 - 7.31 (m, 1H), 7.36 - 7.44 (m, 2H), 7.76 - 7.82 (m, 1H);  $\delta_{\text{C}}$  (126 MHz,  $\text{CDCl}_3$ ) 17.4 (d,  $J$  = 71.8 Hz), 23.5 (d,  $J$  = 67.2 Hz), 30.9, 31.0, 34.9 (d,  $J$  = 3.6 Hz), 35.5 (d,  $J$  = 4.5 Hz), 126.6 (d,  $J$  = 10.9 Hz), 126.6 (d,  $J$  = 9.1 Hz), 129.1 (d,  $J$  = 93.5 Hz), 130.5 (d,  $J$  = 6.4 Hz), 131.9 (d,  $J$  = 2.7 Hz), 150.7 (d,  $J$  = 7.3 Hz);  $\delta_{\text{P}}$  (202 MHz,  $\text{CDCl}_3$ ) 29.14; **GC** tR = 10.66 min; **GC-MS** (EI, 70 eV): m/z (%) = 208 (M<sup>+</sup>) (29), 207 (14), 194 (12), 193 (100), 179 (13), 178 (20), 165 (23), 131 (15), 130 (24), 129 (21), 128 (13), 116 (12), 115 (22), 91 (16), 78 (30), 77 (13), 63 (11). Analytical data are in accordance with those reported in the literature.<sup>9b</sup>

**4.4. 1,3,4-Trimethyl-1,2,3,4-tetrahydrophosphinoline 1-oxide (6).** (2-Hydroxy-3-methylbutyl)methylphenylphosphine oxide (**8**) (0.113 g, 0.50 mmol) was stirred at 170 °C with 73%  $\text{H}_3\text{PO}_4$  (3.285 g, 24.47 mmol) for 21 h. The mixture was cooled below 100 °C and poured on to ice-water (10 mL). The dark brown mixture was extracted with dichloromethane or chloroform (4 x 20 mL). The aqueous solution was washed with sodium hydrogen carbonate solution (10 mL) and water (10 mL). The extracts were dried over  $\text{MgSO}_4$ , filtered, and evaporated under reduced pressure. The residue was purified by column chromatography using AcOEt /MeOH (v/v = 9:1) as eluent yielding a pale yellow oil; yield 0.077 g (6%, isolated as a mixture with 68% of **9**);  $R_f$  = 0.26 (AcOEt/MeOH 9:1);  $\delta_{\text{H}}$  (500 MHz,  $\text{CDCl}_3$ ) (due to overlapping only the selected peaks of epimers are described) 1.07 (d,  $J$  = 7.3 Hz, 3H) and 1.14 (d,  $J$  = 6.9 Hz, 3H) and 1.18 (d,  $J$  = 7.3 Hz, 3H) and 1.21 (d,  $J$  = 6.9 Hz, 3H) and 1.27 (d,  $J$  = 6.9 Hz, 3H) and 1.40 (d,  $J$  = 6.9 Hz, 3H), 1.64 (d,  $J$  = 12.8 Hz, 3H) and 1.67 (d,  $J$  = 12.8 Hz, 3H) and 1.71 (d,  $J$  = 12.8 Hz, 3H), 1.76 - 1.80 (m, 2H), 2.39 - 2.46 (m, 1H), 2.58 - 2.66 (m, 1H), 2.67 - 2.72 (m, 1H), 2.79 - 2.88 (m, 2H), 2.90 - 2.95 (m, 1H);  $\delta_{\text{P}}$  (202 MHz,  $\text{CDCl}_3$ ) 24.40 and 25.57 and 27.43 and 31.07; **GC** peak 1; tR = 10.45 min; **GC-MS** (EI, 70 eV): m/z (%) = 208 (M<sup>+</sup>) (21), 194 (12), 193 (100), 165 (22), 151 (11), 133 (23), 129 (14), 115 (14), 91 (10); **GC** peak 2; tR = 10.64 min; **GC-MS** (EI, 70 eV): m/z (%) = 208 (M<sup>+</sup>) (42), 207 (12), 194 (12), 193 (100), 179 (27), 178 (15), 166 (25); 165 (72), 151 (17), 147 (15); 133 (35), 131 (17), 130 (20), 129 (25), 128 (17), 116 (14), 115 (28), 91 (21); **GC** peak 3; tR = 10.69 min; **GC-MS** (EI, 70 eV): m/z (%) = 208 (M<sup>+</sup>) (38), 194 (12), 193 (100), 179 (26), 178 (10), 166 (35); 165 (90), 151 (20), 147 (13); 133 (41), 131 (14), 130 (20), 129 (25), 128 (16), 116 (10), 115 (23), 91 (18); **GC** peak 4; tR = 10.77 min; **GC-MS** (EI, 70 eV): m/z (%) = 208 (M<sup>+</sup>) (19), 194 (12), 193 (100), 165 (18), 133 (19), 129 (14), 115 (12).

**4.5. (3-methylbut-2-enyl)(methylphenyl)phosphine oxide (10).** To a solution of (2-hydroxy-3-methylbutyl)methylphenylphosphine oxide (**8**) (0.209 g, 0.92 mmol) in dry toluene containing  $\text{Et}_3\text{N}$  (1.876 g, 18.48 mmol) at 0 °C was added mesyl chloride (0.159 g, 1.39 mmol) dropwise. The reaction

was stirred at this temperature for 0.5 hour and then heated to 110 °C and stirred overnight. The reaction mixture was diluted with 1M HCl and extracted with DCM (3×20 mL). The combined organic phases were dried over MgSO<sub>4</sub>, filtered, and evaporated under reduced pressure. The residue was purified by column chromatography using hexane/AcOEt/*i*-PrOH (v/v = 5:1:1) as eluent yielding 0.092 g (48%) of title compound as a pale yellow oil:  $R_f$  = 0.55 (hexane/AcOEt/*i*-PrOH 5:1:1); [Found: C, 69.48; H, 8.51. C<sub>12</sub>H<sub>17</sub>OP requires C, 69.21; H, 8.23%];  $\nu$  max (ATR) 3420, 3054, 2970, 2913, 1438, 1295, 1191, 1115, 902, 747, 698, 502, 432;  $\delta_H$  (500 MHz, CDCl<sub>3</sub>) 1.45 (d,  $J$  = 3.8 Hz, 3H), 1.67 (d,  $J$  = 12.6 Hz, 3H), 1.68 (d,  $J$  = 5.0 Hz, 3H), 2.69 (dd,  $J$  = 15.8, 7.9 Hz, 2H), 5.09 - 5.17 (m, 1H), 7.41 - 7.47 (m, 2H), 7.47 - 7.53 (m, 1H), 7.64 - 7.71 (m, 2H);  $\delta_C$  (126 MHz, CDCl<sub>3</sub>) 14.7 (d,  $J$  = 69.9 Hz), 17.8 (d,  $J$  = 1.8 Hz), 25.7 (d,  $J$  = 2.7 Hz), 32.7 (d,  $J$  = 68.1 Hz), 112.7 (d,  $J$  = 9.1 Hz), 128.4 (d,  $J$  = 10.9 Hz), 130.0 (d,  $J$  = 9.1 Hz), 131.5 (d,  $J$  = 2.7 Hz), 133.5 (d,  $J$  = 95.4 Hz), 137.2 (d,  $J$  = 11.8 Hz);  $\delta_P$  (202 MHz, CDCl<sub>3</sub>) 36.63; GC tR = 9.61 min; GC-MS (EI, 70 eV)  $m/z$  (%) = 208 (M<sup>+</sup>) (17), 140 (100), 139 (30), 125 (68), 77 (22), 51 (12), 47 (22).

4.6. *3-i-propyl-1-methylphosphindoline 1-oxide* (11). (2-Hydroxy-3-methylbutyl)methylphenylphosphine oxide (8) (0.115 g 0.51 mmol) was stirred at 170 °C with 99% H<sub>3</sub>PO<sub>4</sub> (3.091 g, 31.54 mmol) for 21 h. The mixture was cooled below 100 °C and poured on to ice-water (10 mL). The solution was extracted with dichloromethane or chloroform (4 x 20 ml). The aqueous solution was washed with sodium hydrogen carbonate solution (10 mL) and water (10 mL). The extracts were dried over MgSO<sub>4</sub>, filtered, and evaporated under reduced pressure; conversion 3% based on <sup>31</sup>P NMR spectra as a mixture with 9 and 6;  $\delta_P$  (202 MHz, CDCl<sub>3</sub>) 53.55 and 53.91; peak 1: GC tR = 10.03 min; GC-MS (EI, 70 eV)  $m/z$  (%) = 208 (M<sup>+</sup>) (11), 193 (58), 180 (42), 179 (100), 165 (19), 149 (24), 133 (12), 117 (11), 116 (13), 115 (34), 91 (15); peak 2: GC tR = 10.15 min; GC-MS (EI, 70 eV)  $m/z$  (%) = 208 (18), 193 (75), 180 (11), 179 (100), 133 (12), 116 (13), 115 (31), 91 (14).

4.7. (3-Hydroxy-3-methylbutyl)methylphenylphosphine oxide (12). (3-methylbut-2-enyl)(methylphenyl)phosphine oxide (10) (0.059 g, 0.28 mmol) was stirred at 25 °C with 52% H<sub>2</sub>SO<sub>4</sub> (3.38 g, 17.85 mmol) for 4 hours. The pale yellow mixture was poured on to ice water (10 mL). The solution was extracted with dichloromethane or chloroform (4x20 ml). The extracts were dried over MgSO<sub>4</sub>, filtered, and evaporated under reduced pressure. The residue was purified by column chromatography using AcOEt/MeOH (v/v = 9:1) as eluent yielding 0.040 g (63%) of title compound as a colorless oil:  $R_f$  = 0.37 (AcOEt/MeOH 9:1); [Found: C, 63.94; H, 8.69. C<sub>12</sub>H<sub>19</sub>O<sub>2</sub>P requires C, 63.70; H, 8.46%];  $\nu$  max (ATR) 3320, 2964, 1437, 1296, 1262, 1170, 1152, 1029, 917, 877, 808, 740, 697, 502;  $\delta_H$  (500 MHz, CDCl<sub>3</sub>) 1.19 (d,  $J$  = 1.6 Hz, 6H), 1.58 - 1.69 (m, 1H), 1.71 (d,  $J$  = 12.9 Hz, 3H), 1.73 - 1.83 (m, 1H), 1.96 - 2.16 (m, 2H), 3.32 (bs., 1H), 7.43 - 7.55 (m, 3H), 7.65 - 7.74 (m, 2H);  $\delta_C$  (126 MHz, CDCl<sub>3</sub>) 16.0 (d,  $J$  = 70.8 Hz), 26.4 (d,  $J$  = 70.8 Hz), 28.9, 29.1, 35.1 (d,  $J$  = 3.6 Hz), 69.5 (d,  $J$  = 10.9 Hz), 128.6 (d,  $J$  = 10.9 Hz), 130.0 (d,  $J$  = 9.1 Hz), 131.6 (d,  $J$  = 2.7 Hz), 133.1 (d,  $J$

= 96.3 Hz);  $\delta_P$  (202 MHz,  $CDCl_3$ ) 39.88; GC tR = 10.29 min; GC-MS (EI, 70 eV) m/z (%) = 211 ( $M^+ - CH_3$ ) (30), 208 ( $M^+ - H_2O$ ) (3), 168 (11), 141 (29), 140 (100), 139 (14), 125 (36), 77 (18), 59 (19), 47 (22). Analytical data are in accordance with those reported in the literature.<sup>9</sup>

**4.8. (3-methylbut-1-enyl)(methylphenyl)phosphine oxide (13).** To a solution of (2-hydroxy-3-methylbutyl)methylphenylphosphine oxide (**8**) (0.209 g, 0.92 mmol) in dry toluene containing  $Et_3N$  (1.876 g, 18.48 mmol) at 0 °C was added mesyl chloride (0.159 g, 1.39 mmol) dropwise. The reaction was stirred at this temperature for 0.5 hour and then heated to 110 °C and stirred overnight. The reaction mixture was diluted with 1M HCl and extracted with DCM (3×20 mL). The combined organic phases were dried over  $MgSO_4$ , filtered, and evaporated under reduced pressure. The residue was purified by column chromatography using hexane/AcOEt/*i*-PrOH (v/v = 5:1:1) as eluent yielding 0.040 g (21%) of title compound as a pale yellow oil:  $R_f$  = 0.64 (hexane/AcOEt/*i*-PrOH 5:1:1); [Found: C, 69.38; H, 8.42.  $C_{12}H_{17}OP$  requires C, 69.21; H, 8.23%];  $\nu_{max}$  (ATR) 3425, 2961, 2926, 2869, 1627, 1437, 1295, 1195, 1116, 990, 900, 744, 698, 509;  $\delta_H$  (500 MHz,  $CDCl_3$ ) 1.02 - 1.06 (m, 6H), 1.73 (d,  $J$  = 13.2 Hz, 3H), 2.41 - 2.50 (m, 1H), 5.86 - 5.96 (m, 1H), 6.61 - 6.71 (m, 1H), 7.43 - 7.52 (m, 3H), 7.67 - 7.73 (m, 2H);  $\delta_C$  (126 MHz,  $CDCl_3$ ) 16.9 (d,  $J$  = 74.5 Hz), 21.0, 32.6 (d,  $J$  = 16.3 Hz), 120.1 (d,  $J$  = 99.9 Hz), 128.5 (d,  $J$  = 11.8 Hz), 130.0 (d,  $J$  = 9.1 Hz), 131.4 (d,  $J$  = 2.7 Hz), 134.2 (d,  $J$  = 101.7 Hz), 156.8;  $\delta_P$  (202 MHz,  $CDCl_3$ ) 26.67; GC tR = 9.42 min; GC-MS (EI, 70 eV) m/z (%) = 208 ( $M^+$ ) (25), 207 (14), 193 (13), 165 (28), 140 (100), 139 (25), 131 (14), 125 (76), 91 (17).

### Supplementary data

Supplementary data ( $^1H$ ,  $^{13}C$  and  $^{31}P$  NMR spectras of the products) associated with this article can be found in the online version, at <http://dx.doi.org/10.1016/....>

### Acknowledgments

Financial support from National Science Centre (SONATA-BIS funding scheme, grant no. 2012/07/E/ST5/00544) is kindly acknowledged.

### Notes and references

1. a) A. Orita, J. Yaruva, J. Otera, *Angew. Chem. Int. Ed.* 1999, **38**, 2267–2270; b) M. Modjewski, S. V. Lindeman, R. Rathore, *Org. Lett.* 2009, **11**, 4656–4659; c) S. Nagumo, T. Miura, M. Mizukami, I. Miyoshi, M. Imai, N. Kawahara, H. Akita, *Tetrahedron* 2009, **65**, 9884–9896; d) M. Oliverio, M. Nardi, P. Constanzo, L. Cariati, G. Cravotto, S. V. Giofre, A. Procopio, *Molecules* 2014, **19**, 5599–5610.

2. a) C. J. Barrow, S. T. Bright, J. M. Coxon, P. J. Steel, *J. Org. Chem.* 1989, **54**, 2542–2549; b) M. D. Reeder, G. S. C. Srikanth, S. B. Jones, S. L. Castle, *Org. Lett.* 2005, **7**, 1089–1092; a) N. Ahmed, G. K. Pathe, B. Venkata, *Tetrahedron Lett.* 2014, **55**, 3683–3687.
3. a) B. L. Shapiro, M. J. Shapiro, *J. Org. Chem.* 1976, **41**, 1522–1529; b) W. Wysocka, P. Canonne, L. C. Leitch, *Synthesis* 1977, 261–263; c) S. Shiotani, H. Okada, T. Yaroamoto, K. Nakamata, J. Adachi, H. Nakamoto, *Heterocycles* 1996, **43**, 113–126.
4. a) J. Malthete, J. Canceill, J. Gabard, J. Jacques, *Tetrahedron* 1981, **37**, 2823–2828; b) H. Hara, S. Komoriya, T. Miyashita, O. Hoshino, *Tetrahedron: Asymmetry* 1995, **6**, 1683–1692; c) L. G. Meimetis, M. Nodwell, L. Yang, X. Wang, B. O. Patrick, R. J. Andersen, J. Wu, C. Harwig, G. R. Stenton, L. F. MacKenzie, T. MacRury, A. Ming-Lum, C. J. Ong, A. L.-F. Mui, G. Krystal, *Eur. J. Org. Chem.* 2012, 5195–5207.
5. a) J. J. Parlow, M. D. Mahoney, *Pestic. Sci.* 1996, **46**, 227–235; b) Y. Endo, S. Takehana, M. Ohno, P. E. Driedger, S. Stabel, M. Y. Mizutani, N. Tomioka, A. Itai, K. Shudo, *J. Med. Chem.* 1998, **41**, 1476–1496; c) M. Asim, D. Klonowska, C. Choueiri, I. Korobkov, K. E. Carlson, J. A. Katzenellenbogen, T. Durst, *Bioorg. Med. Chem. Lett.* 2012, **22**, 3713–3717.
6. a) S. Das, A. K. Saha, D. Mukherjee, *Tetrahedron Lett.* 1994, **35**, 4027–4030; b) M. Medjahdi, J. C. Golzalez-Gomez, F. Foubelo, M. Yus, *Eur. J. Org. Chem.* 2011, 2230–2234; c) D. C. Braddock, J. S. Marklew, A. J. F. Thomas, *Chem. Commun.* 2011, **47**, 9051–9053.
7. a) H. Hara, O. Hoshino, B. Umezawa, Y. Iitaka, *J. Chem. Soc., Perkin Trans. 1* 1979, 2657–2663; b) E. J. Corey, G. Luo, L. S. Lin, *Angew. Chem. Int. Ed.* 1998, **37**, 1126–1128; c) H. Zhai, S. Luo, C. Ye, Y. Ma, *J. Org. Chem.*, 2003, **68**, 8268–8271; d) D. Chen, H.-M. Liu, M.-M. Li, Y.-M. Yan, W.-D. Xu, X.-N. Li, Y.-X. Cheng, H.-B. Qin, *Chem. Commun.* 2015, **51**, 14594–14596.
8. a) G. A. Dilbeck, D. L. Morris, K. D. Berlin, *J. Org. Chem.* 1975, **40**, 1150–1157; b) M. El-Deek, G. D. Macdonell, S. D. Venkataramu, K. D. Berlin, *J. Org. Chem.* 1976, **41**, 1403–1407; c) N. Gurusamy, K. D. Berlin, D. van der Helm, M. B. Hossain, *J. Am. Chem. Soc.* 1982, **104**, 3107–3114; d) A. S. Bogachenkov, A. V. Dogadina, V. P. Boyarskiy, A. V. Vasilyev, *Org. Biomol. Chem.* 2015, **13**, 1333–1338.
9. a) J. I. Grayson, H. K. Norrish, S. Warren, *J. Chem. Soc., Perkin Trans. 1* 1976, 2556–2562; b) P. G. Edwards, S. J. Paisey, R. P. Tooze, *J. Chem. Soc., Perkin Trans. 1* 2000, 3122–3128.
10. K. Włodarczyk, M. Stankevič, *Tetrahedron* 2016, **72**, 5074–5090.
11. a) I. Granoth, J. C. Martin, *J. Am. Chem. Soc.* 1981, **103**, 2711–2715; b) Y. Yamamoto, K. Nakao, T. Hashimoto, S. Matsukawa, N. Suzukawa, S. Kojima, K. Akiba, *Heteroatom Chem.* 2011, **22**, 523–530;
12. R.G. Parr, W. Yang, *Density-Functional Theory of Atoms and Molecules*, Oxford University Press, New York, 1989.
13. A. D. Becke, *J. Chem. Phys.* 1993, **98**, 5648–5652.

14. a) R. Krishnan, J. S. Binkley, R. Seeger, J. A. Pople, *J. Chem. Phys.* 1980, **72**, 650–654; b) M. J. Frisch, J. A. Pople, J. S. Binkley, *J. Chem. Phys.* 1984, **80**, 3265–3269.
15. a) J. Baker, K. Wolinski, M. Malagoli, D. Kinghorn, P. Wolinski, G. Magyarfalvi, S. Saebo, T. Janowski, P. Pulay, *J. Comput. Chem.* 2009, **30**, 317–335; b) PQS version 4.0, Parallel Quantum Solutions, 2013 Green Acres Road, Fayetteville, Arkansas 72703.
16. a) A. Klamt, G. Schüürmann, *J. Chem. Soc. Perkin Trans. 2* 1993, 799-805. b) J. Andzelm, C. Kölmel, A. Klamt, *J. Chem. Phys.* 1995, **103**, 9312-9320. c) A. Klamt, *J. Phys. Chem.* 1995, **99**, 2224-2235. d) A. Klamt, V. Jonas, *J. Chem. Phys.* 1996, **105**, 9972-9981. e) K. Baldrige, A. Klamt, *J. Chem. Phys.* 1997, **106**, 6622-6633.